Endocrinology, 2024, **165**, 1–12
https://doi.org/10.1210/endocr/bqad185
Advance access publication 6 December 2023
Research Article

Vasoinhibin's Apoptotic, Inflammatory, and Fibrinolytic Actions Are in a Motif Different From Its Antiangiogenic HGR Motif

Juan Pablo Robles,[1,2,*] Magdalena Zamora,[1,*] Jose F. Garcia-Rodrigo,[1] Alma Lorena Perez,[1] Thomas Bertsch,[3] Gonzalo Martinez de la Escalera,[1] Jakob Triebel,[3] and Carmen Clapp[1]

[1]Instituto de Neurobiología, Universidad Nacional Autónoma de México (UNAM), Querétaro 76230, México
[2]VIAN Therapeutics, Inc., San Francisco, CA 94107, USA
[3]Laboratory Medicine and Transfusion Medicine, Institute for Clinical Chemistry, Nuremberg General Hospital & Paracelsus Medical University, Nuremberg 90419, Germany

Correspondence: Juan Pablo Robles, MSc, PhD, Instituto de Neurobiología, Universidad Nacional Autónoma de México (UNAM), Campus UNAM-Juriquilla, Blvd. Juriquilla 3001, Querétaro 76230, México.
Email: jp.robles@viantx.com.
*Equal contribution

Abstract

Vasoinhibin, a proteolytic fragment of the hormone prolactin, inhibits blood vessel growth (angiogenesis) and permeability, stimulates the apoptosis and inflammation of endothelial cells, and promotes fibrinolysis. The antiangiogenic and antivasopermeability properties of vasoinhibin were recently traced to the HGR motif located in residues 46 to 48 (H46-G47-R48), allowing the development of potent, orally active, HGR-containing vasoinhibin analogues for therapeutic use against angiogenesis-dependent diseases. However, whether the HGR motif is also responsible for the apoptotic, inflammatory, and fibrinolytic properties of vasoinhibin has not been addressed. Here, we report that HGR-containing analogues are devoid of these properties. Instead, the incubation of human umbilical vein endothelial cells with oligopeptides containing the sequence HNLSSEM, corresponding to residues 30 to 36 of vasoinhibin, induced apoptosis, nuclear translocation of NF-κB, expression of genes encoding leukocyte adhesion molecules (*VCAM1* and *ICAM1*) and proinflammatory cytokines (*IL1B, IL6,* and *TNF*), and adhesion of peripheral blood leukocytes. Also, intravenous or intra-articular injection of HNLSSEM-containing oligopeptides induced the expression of *Vcam1, Icam1, Il1b, Il6,* and *Tnf* in the lung, liver, kidney, eye, and joints of mice and, like vasoinhibin, these oligopeptides promoted the lysis of plasma fibrin clots by binding to plasminogen activator inhibitor-1 (PAI-1). Moreover, the inhibition of PAI-1, urokinase plasminogen activator receptor, or NF-κB prevented the apoptotic and inflammatory actions. In conclusion, the functional properties of vasoinhibin are segregated into 2 different structural determinants. Because apoptotic, inflammatory, and fibrinolytic actions may be undesirable for antiangiogenic therapy, HGR-containing vasoinhibin analogues stand as selective and safe agents for targeting pathological angiogenesis.

Key Words: endothelial cell, inflammation, apoptosis, fibrinolysis, vasoinhibin, HGR

Abbreviations: bFGF, basic fibroblast growth factor; BSA, bovine serum albumin; CRIVi45-51, cyclic retro-inverse-vasoinhibin analogue; ECGS, endothelial cell growth supplement; ELISA, enzyme-linked immunosorbent assay; FBS, fetal bovine serum; HUVEC, human umbilical vein endothelial cells; ICAM1, intercellular adhesion molecule 1; IL-, interleukin; PAI-1, plasminogen activator inhibitor-1 PBS phosphate-buffered saline; PBST, phosphate buffered saline with 0.1% Tween-20; PCR, polymerase chain reaction; PRL, prolactin; TNF, tumor necrosis factor; tPA, tissue plasminogen activator; uPA, urokinase plasminogen activator; uPAR, urokinase plasminogen activator receptor; VCAM1, vascular cell adhesion molecule 1; VEGF, vascular endothelial growth factor; Vi1-123, 123-residue vasoinhibin (1-123); Vi1-48, 48-residue vasoinhibin (1-48); Vi45-51, linear vasoinhibin analogue (45-51).

The formation of new blood vessels (angiogenesis) underlies the growth and repair of tissues and, when exacerbated, contributes to multiple diseases, including cancer, vasoproliferative retinopathies, and rheumatoid arthritis (1). Antiangiogenic therapies based on tyrosine kinase inhibitors (2, 3) and monoclonal antibodies against vascular endothelial growth factor (VEGF) or its receptor (4) have proven beneficial for the treatment of cancer and retinal vasoproliferative diseases (5). However, disadvantages such as toxicity (6-8) and resistance (9) have incentivized the development of new treatments.

Vasoinhibin is a proteolytically generated fragment of the hormone prolactin that inhibits endothelial cell proliferation, migration, permeability, and survival (10). It binds to a multi-component complex formed by plasminogen activator inhibitor-1 (PAI-1), urokinase plasminogen activator (uPA), and the uPA receptor on endothelial cell membranes, which can contribute to the inhibition of multiple signaling pathways (Ras-Raf-MAPK, Ras-Tiam1-Rac1-Pak1, PI3K-Akt, and PLCγ-IP_3-eNOS) activated by several proangiogenic and vasopermeability factors (VEGF, basic fibroblast growth factor [bFGF], bradykinin, and interleukin [IL]-1β) (10).

Received: 21 August 2023. **Editorial Decision:** 30 November 2023. **Corrected and Typeset:** 23 December 2023

Moreover, vasoinhibin, by itself, activates the NF-κB pathway in endothelial cells to stimulate apoptosis (11) and trigger the expression of inflammatory factors and adhesion molecules, resulting in leukocyte infiltration (12). Finally, vasoinhibin promotes the lysis of a fibrin clot by binding to PAI-1 and inhibiting its antifibrinolytic activity (13).

The antiangiogenic determinant of vasoinhibin was recently traced to a short linear motif of just 3 amino acids (His46-Gly47-Arg48) (the HGR motif), which led to the development of heptapeptides comprising residues 45 to 51 of vasoinhibin that inhibited angiogenesis and vasopermeability with the same potency as whole vasoinhibin (14) (Fig. 1A). The linear vasoinhibin analogue (Vi45-51) was then optimized into a fully potent, proteolysis-resistant, orally active cyclic retro-inverse heptapeptide (CRIVi45-51) (Fig. 1A) for the treatment of angiogenesis-dependent diseases (14). Notably, thrombin generates a vasoinhibin of 48 amino acids (Vi1-48) that contains the HGR motif (Fig. 1A). Vi1-48 is antiangiogenic and fibrinolytic (15), suggesting that the HGR motif could also be responsible for the apoptotic, inflammatory, and fibrinolytic properties of vasoinhibin. This possibility needed to be analyzed to support the therapeutic future of the HGR-containing vasoinhibin analogues as selective and safe inhibitors of blood vessel growth and permeability. Moreover, the identification of specific functional domains within the vasoinhibin molecule provides insights and tools for understanding its overlapping roles in angiogenesis, inflammation, and coagulation under health and disease.

Materials and Methods

Reagents

Six linear oligopeptides (>95% pure) acetylated and amidated at the N- and C-termini, respectively (Table 1), the linear (Vi45-51), and the cyclic-retro-inverse-vasoinhibin-(45-51)-peptide (CRIVi45–51) were synthesized by GenScript (Piscataway, NJ). Recombinant vasoinhibin isoforms of 123 (Vi1-123) (16) or 48 residues (Vi1-48) (15) were produced as reported. Recombinant human prolactin (PRL) was provided by Michael E. Hodsdon (17) (Yale University, New Haven, CT). Human recombinant plasminogen activator inhibitor 1 (PAI-1) was from Thermo Fisher Scientific (Waltham, MA), and human tissue plasminogen activator (tPA) from Sigma Aldrich (St. Louis, MO). Rabbit monoclonal anti-PAI-1 [EPR17796] (ab187263, RRID:AB_2943367) and rabbit polyclonal anti-β-tubulin antibodies (Cat# ab6046, RRID: AB_2210370) were purchased from Abcam (Cambridge, UK), and mouse monoclonal anti-uPA receptor (anti-uPAR) from R&D systems (Minneapolis, MN, Cat# MAB807, RRID: AB_2165463). The NF-κB activation inhibitor BAY 11-7085 and lipopolysaccharides (LPS) from *Escherichia coli* O55:B5 were from Sigma Aldrich. Recombinant human vascular endothelial growth factor-165 (VEGF) was from GenScript, and basic fibroblast growth factor (bFGF) was donated by Scios, Inc. (Mountain View, CA).

Cell Culture

Human umbilical vein endothelial cells (HUVEC) were isolated (18) and cultured in F12K medium supplemented with 20% fetal bovine serum (FBS), 100 μg mL^{-1} heparin

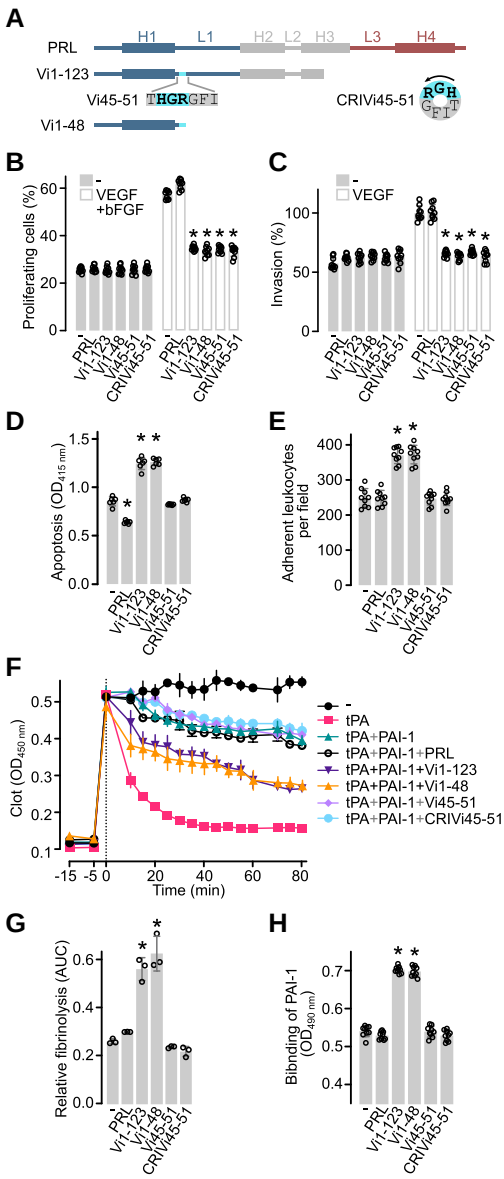

Figure 1. HGR-containing vasoinhibin analogues are neither inflammatory, apoptotic, nor fibrinolytic. (A) Diagram of the secondary structure of prolactin with 199 residues (PRL), the 123-residue (Vi1-123), and the 48-residue (Vi1-48) vasoinhibin isoforms. The location and sequence of the linear HGR-containing vasoinhibin analogue (Vi45-51) and the cyclic retro-inverse HGR-containing vasoinhibin analogue (CRIVi45-51) are illustrated. The antiangiogenic HGR motif is indicated in bold. (B) Effect of 100 nM PRL, Vi1-123, Vi1-48, Vi45-51, or CRIVi45-51 on the proliferation of HUVEC in the presence or absence of 25 ng mL^{-1} VEGF and 20 ng mL^{-1} bFGF. Values are means ± SD relative to total cells ($n = 9$). (C) Effect of 100 nM PRL, Vi1-123, Vi1-48, Vi45-51, or CRIVi45-51 on the invasion of HUVEC in the presence or absence of 50 ng mL^{-1} VEGF. Values are means ± SD relative to VEGF stimulated values ($n = 9$). *$P < .0001$ vs VEGF + bFGF (–) or VEGF (–) controls (2-way ANOVA, Dunnett's). (D) Apoptosis of HUVEC in the absence (–) or presence of 100 nM of PRL, Vi1-123, Vi1-48, Vi45-51, or CRIVi45-51 ($n = 6$). (E) Leukocyte adhesion to a HUVEC monolayer in the absence (–) or presence of 100 nM of PRL, Vi1-123, Vi1-48, Vi45-51, or CRIVi45-51 ($n = 9$). (F) Lysis of a plasma clot by tissue plasminogen activator (tPA) alone or together with the plasminogen activator inhibitor-1 (PAI-1) in the presence or absence of PRL, Vi1-123, Vi1-48, Vi45-51, or CRIVi45-51 ($n = 3$). (G) Fibrinolysis relative to tPA and tPA + PAI-1 calculated with the area under the curve (AUC) of (F). (H) Binding of PAI-1 to immobilized PRL, Vi1-123, Vi1-48, Vi45-51, or CRIVi45-51 in an ELISA-based assay ($n = 6$). Individual values are shown with open circles. Values are means ± SD, *$P < .001$ vs control without treatment (–) (1-way ANOVA, Dunnett's).

Table 1. Synthetic oligopeptides

IUPAC Name	Alias	Sequence	Molecular mass (Da)
Vasoinhibin-(45-51)-peptide	Vi45-51	THGRGFI	827.93
Vasoinhibin-(1-15)-peptide	1-15	LPICPGGAARCQVTL	1497.87
Vasoinhibin-(12-25)-peptide	12-25	QVTLRDLFDRAVVL	1685.97
Vasoinhibin-(20-35)-peptide	20-35	DRAVVLSHYIHNLSSE	1881.06
Vasoinhibin-(30-45)-peptide	30-45	HNLSSEMFSEFDKRYT	2032.20
Vasoinhibin-(35-48)-peptide	35-48	EMFSEFDKRYTHGR	1844.02

(Sigma Aldrich), 25 μg mL^{-1} endothelial cell growth supplement (ECGS) (Corning, Glendale, AZ), and 100 U mL^{-1} penicillin-streptomycin.

Cell Proliferation

HUVEC were seeded at 14 000 cells cm^{-2} in a 96-well plate and, after 24 hours, starved with 0.5% FBS, F12K for 12 hours. Treatments were added in 20% FBS, F12K containing 100 μg mL^{-1} heparin for 24 hours and consisted of 25 ng mL^{-1} VEGF and 20 ng mL^{-1} bFGF alone or in combination with 100 nM PRL (as negative control), 123-residue vasoinhibin (Vi1-123) or 48-residue vasoinhibin (Vi1-48) (positive controls), linear vasoinhibin analogue (Vi45-51), cyclic retro-inverse-vasoinhibin analogue (CRIVi45-51), synthetic oligopeptides mapping region 1 to 48 of vasoinhibin (1-15, 12-25, 20-35, 30-45, or 35-48). DNA synthesis was quantified by the DNA incorporation of the thymidine analogue 5-ethynyl-2′-deoxyuridine (EdU; Sigma Aldrich) (10 μM) added at the time of treatments and labeled by the click reaction with Azide Fluor 545 (Sigma Aldrich) as reported (14, 19). Total HUVEC were counterstained with Hoechst 33342 (Sigma Aldrich). Images were obtained in a fluorescence-inverted microscope (Olympus IX51, Japan) and quantified using CellProfiler software (20).

Cell Invasion

HUVEC invasion was evaluated using the Transwell Matrigel barrier assay (21). HUVEC were seeded at 28 000 cells cm^{-2} on the luminal side of an 8-μm-pore insert of a 6.5 mm Transwell (Corning) precoated with 0.38 mg mL^{-1} Matrigel (BD Biosciences, San Jose, CA) in starvation medium (0.5% FBS F12K, without heparin or ECGS). Treatments were added inside the Transwell and consisted of 100 nM PRL, Vi1-123, Vi1-48, Vi45-51, CRIVi45-51, or the oligopeptides 1-15, 12-25, 20-35, 30-45, or 35-48. Conditioned medium of 3T3L1 cells (ATCC, Manassas, VA) cultured for 2 days in 10% FBS was filtered (0.22 μm), supplemented with 50 ng mL^{-1} VEGF, and placed in the lower chamber as chemoattractant. Sixteen hours later, cells invading the bottom of the Transwell were fixed, permeabilized, Hoechst-stained, and counted using the CellProfiler software (20).

Leukocyte Adhesion Assay

HUVEC were seeded on a 96-well plate and grown to confluency. HUVEC monolayers were treated for 16 hours with 100 nM PRL, Vi1-123, Vi1-48, Vi45-51, CRIVi45-51, or the oligopeptides 1-15, 12-25, 20-35, 30-45, 35-48 in 20% FBS, F12K without heparin or ECGS. Treatments were added alone or in combination with anti-PAI-1 (5 μg mL^{-1}), anti-uPAR (5 μg mL^{-1}), or anti-β-tubulin (5 μg mL^{-1}) antibodies. NF-κB activation inhibitor BAY 11-7085 (5 μM) was added 30 minutes prior to treatments. After the 16-hour treatment, HUVEC were exposed to a leukocyte preparation obtained as follows. Briefly, whole blood was collected into EDTA tubes, centrifuged (300*g* for 5 minutes), and the plasma layer discarded. The remaining cell pack was diluted 1:10 in red blood lysis buffer (150 mM NH_4Cl, 10 mM $NaHCO_3$, and 1.3 mM EDTA disodium) and rotated for 10 minutes at room temperature. The tube was centrifuged (300*g* 5 minutes), and when erythrocytes were no longer visible, leukocytes were collected by discarding the supernatant. Leukocytes were washed with cold phosphate buffered saline (PBS) followed by another centrifugation step (300*g* 5 minutes) and resuspended in 5 mL of 5 μg mL^{-1} of Hoechst 33342 (Thermo Fisher Scientific) diluted in warm PBS. Leukocytes were incubated under 5% CO_2-air at 37 °C for 30 minutes, washed with PBS 3 times, and resuspended into 20% FBS, F12K to 10^6 leukocytes mL^{-1}. The medium of HUVEC was replaced with 100 μL of Hoechst-stained leukocytes (10^5 leukocytes per well) and incubated for 1 hour at 37 °C. Finally, HUVEC were washed 3 times with warm PBS, and images were obtained in an inverted fluorescent microscope (Olympus IX51) and quantified using the CellProfiler software (20).

Apoptosis

HUVEC grown to 80% confluency on 12-well plates were incubated under starving conditions (0.5% FBS F12K) for 4 hours. Then, HUVEC were treated for 24 hours with 100 nM PRL, Vi1-123, Vi1-48, Vi45-51, CRIVi45-51, or the oligopeptides 1-15, 12-25, 20-35, 30-45, or 35-48 in 20% FBS, F12K without heparin or ECGS. Treatments were added alone or in combination with anti-PAI-1 (5 μg mL^{-1}), anti-uPAR (5 μg mL^{-1}), or anti-β-tubulin (5 μg mL^{-1}) antibodies. NF-κB activation inhibitor BAY 11-7085 (5 μM) was added 30 minutes before treatments. Apoptosis was evaluated using the cell death detection enzyme-linked immunosorbent assay (ELISA) kit (Roche, Basel, Switzerland). HUVEC were trypsinized, centrifuged, and resuspended with incubation buffer to 10^5 cells mL^{-1}. Cells were incubated at room temperature for 30 minutes and centrifugated at 20 000*g* for 10 minutes (Avanti J-30I Centrifuge, Beckman Coulter, Brea, CA). The supernatant was collected and diluted 1:5 with incubation buffer (final concentration ~20 000 cells mL^{-1}). HUVEC concentration was standardized, and the assay was carried out according to the manufacturer's instructions, measuring absorbance at 415 nm.

Fibrinolysis Assay

Human blood was collected into a 3.2% sodium citrate tube (BD Vacutainer) and centrifugated (1200*g* for 10 minutes at 4 °C) to

obtain plasma. Plasma (24 μL) was added to a 96-well microplate containing 20 μL of 50 mM $CaCl_2$. Turbidity was measured as an index of clot formation by monitoring absorbance at 405 nm every 5 minutes after plasma addition. Before adding plasma, 0.5 μM of PAI-1 was preincubated in 10 mM Tris–0.01% Tween 20 (pH 7.5) at 37 °C for 10 minutes alone or in combination with 3 μM Vi1-123, Vi1-48, Vi45-51, CRIVi45-51, or the oligopeptides 1-15, 12-25, 20-35, 30-45, or 35-48. Once the clot was formed (~20 minutes and maximum absorbance), treatments were added to a final concentration per well of 24% v/v plasma, 10 mM $CaCl_2$, 60 pM human tissue plasminogen activator (tPA), 0.05 μM PAI-1, and 0.3 μM Vi1-123, Vi1-48, Vi45-51, CRIVi45-51, or the oligopeptides 1-15, 12-25, 20-35, 30-45, or 35-48. Absorbance (405 nm) was measured every 5 minutes to monitor clot lysis.

PAI-1 Binding Assay

A 96-well ELISA microplate was coated overnight at 4 °C with 50 μL of 6.25 μM PRL, Vi1-123, Vi1-48, Vi45-51, CRIVi45-51, or the oligopeptides 1-15, 12-25, 20-35, 30-45, or 35-48, diluted in PBS. Microplate was blocked for 1 hour at room temperature with 5% w/v nonfat dry milk in 0.1% Tween-20-PBS (PBST), followed by 3 washes with PBST. Next, 100 nM of PAI-1 diluted in 0.2 mg mL^{-1} bovine serum albumin (BSA)-PBST was added and incubated for 1 hour at room temperature, followed by a 3-wash step with PBST. Anti-PAI-1 antibodies (1 μg mL^{-1} diluted in blocking buffer) were added and incubated for 1 hour at room temperature. Microplates were then washed 3 times with PBST, and goat anti-rabbit HRP antibody (Jackson ImmunoResearch Labs, West Grove, PA, Cat# 111-035-144, RRID:AB_2307391) at 1:2500 (diluted in 50% blocking buffer and 50% PBS) added and incubated for 1 hour at room temperature. Three last washes were done with PBST and microplates incubated for 30 minutes under darkness with 100 μL per well of an o-phenylenediamine dihydrochloride (OPD) substrate tablet diluted in 0.03% H_2O_2 citrate buffer (pH 5). Finally, the reaction was stopped with 50 μL of 3 M HCl, and absorbance measured at 490 nm.

NF-κB Nuclear Translocation Assay

HUVEC were seeded on 1 μg cm^{-2} fibronectin-coated 18 mm-coverslips placed in 12-well plates and grown in complete media to 80% confluence. Then, cells were treated, under starving conditions (0.5% FBS F12K), with 100 nM PRL, Vi1-123, Vi1-48, Vi45-51, CRIVi45-51, or the oligopeptides 20-35 or 30-45. After 30 minutes, cells were washed with PBS, fixed with 4% of paraformaldehyde (30 minutes), permeabilized with 0.5% Triton-X (Tx)-100 in PBS (30 minutes), blocked with 5% normal goat serum, 1% BSA, 0.05% Tx-100 in PBS (1 hour), and incubated with 1:200 anti-NF-κB p65 antibodies (Santa Cruz Biotechnology, Santa Cruz, CA, Cat# sc-8008, RRID:AB_628017) in 1% BSA, 0.1% Tx-100 PBS overnight in a humidity chamber at 4 °C. HUVEC were washed and incubated with 1:500 goat anti-mouse secondary antibodies coupled to Alexa fluor 488 (Abcam, Cambridge, UK, Cat# ab150113, RRID: AB_2576208) in 1% BSA, 0.1% Tx-100 PBS (2 hours in darkness). Nuclei were counterstained with 5 μg mL^{-1} Hoechst 33342 (Sigma-Aldrich). Coverslips were mounted with Vectashield (Vector Laboratories, Burlingame, CA) and digitalized under fluorescence microscopy (Olympus IX51).

Quantitative Polymerase Chain Reaction of HUVECs

HUVEC at 80% confluency in 6-well plates under starving conditions (0.5% FBS F12K) were treated for 4 hours with 100 nM PRL, Vi1-123, Vi1-48, Vi45-51, CRIVi45-51, or the oligopeptides 1-15, 12-25, 20-35, 30-45, or 35-48. RNA was isolated using TRIzol (Invitrogen) and retrotranscribed with the high-capacity cDNA reverse transcription kit (Applied Biosystems). Polymerase chain reaction (PCR) products were obtained and quantified using Maxima SYBR Green qPCR Master Mix (Thermo Fisher Scientific) in a final reaction containing 20 ng of cDNA and 0.5 μM of each of the following primer pairs for human genes: *ICAM1* (5′-GTGACCGTGAATGTGCTCTC-3′ and 5′-CCTGCAGTGCCCATTATGAC-3′), *VCAM1* (5′-GCACTGGGTTGACTTTCAGG-3′ and 5′-AACATCTCCGTACCATGCCA-3′), *IL1A* (5′-ACTGCCCAAGATGAAGACCA-3′ and 5′-TTAGTGCCGTGAGTTTCCCA-3′), *IL1B* (5′-GGAGAATGACCTGAGCACCT-3′ and 5′GGAGGTGGAGAGCTTTCAGT-3′), *IL6* (5′-CCTGATCCAGTTCCTGCAGA-3′ and 5′-CTACATTTGCCGAAGAGCCC-3′), *TNF* (5′-ACCACTTCGAAACCTGGGAT-3′ and 5′-TCTTCTCAAGTCCTGCAGCA-3′) were quantified relative to *GAPDH* (5′-GAAGGTCGGAGTCAACGGATT-3′ and 5′-TGACGGTGCCATGGAATTTG-3′). Amplification consisted of 40 cycles of 10 seconds at 95 °C, 30 seconds at the annealing temperature of each primer pair, and 30 seconds at 72 °C. The mRNA expression levels were calculated by the $2^{-\Delta\Delta CT}$ method.

Animals

C57BL6 mice were housed under standard laboratory conditions. Experiments were approved by the Bioethics Research Committee of the Institute of Neurobiology of the National University of Mexico (UNAM) in compliance with the US National Research Council's Guide for the Care and Use of Laboratory Animals (8th ed, National Academy Press, Washington, DC).

In Vivo Vascular Inflammation

Vascular inflammation was evaluated as previously reported (22). Briefly, female C57BL6 mice (8 weeks old) were injected intravenously with 16.6 μg of Vi45-51 or 40.7 μg of 30-45 in 50 μL of PBS to achieve ~10 μM in serum. Controls were injected intravenously with 50 μL PBS. After 2 hours, animals were euthanized by cervical dislocation and perfused intracardially with PBS. A fragment of the lungs, liver, kidneys, and whole eyes were dissected and placed immediately in TRIzol reagent and retrotranscribed. The expression of *Icam1*, *Vcam1*, *Il1b*, *Il6*, and *Tnf* were quantified relative to *Gapdh* by quantitative PCR as indicated for HUVEC using the following primer pairs for the mouse genes: *Icam1* (5′-GCTGGGATTCACCTCAAGAA-3′ and 5′-TGGGGACACCTTTTAGCATC-3′), *Vcam1* (5′-ATTGGGAGAGACAAAGCAGA-3′ and 5′-GAAAAAGAAGGGGAGTCACA-3′), *Cd45* (5′-TATCGCGGTGTAAAACTCGTCA-3′ and 5′-GCTCAGGCCAAGAGACTAACGT-3′), *Il1b* (5′-GTTGATTCAAGGGGACATTA-3′ and 5′-AGCTTCAATGAAAGACCTCA-3′), *Il6* (5′-GAGGATACCACTCCCAACAGACC-3′ and 5′-AAGTGCATCATCGTTGTTCATACA-3′), and *Tnf* (5′-CATCTTCTCAAAATTCGAGTGACAA-3′ and 5′-TGGGAGTAGACAAGGTACAACCC-3′).

Joint Inflammation

Male C57BL/6 mice (8 weeks old) were injected into the articular space of knee joints with vehicle (saline), or 87 pmol of Vi45-51 (72 ng) or 30-45 (176.8 ng) in a final volume of 10 µL saline. Twenty-four hours after injections, animals were euthanized in a CO_2-saturated atmosphere. Joints were extracted, pulverized with nitrogen, RNA extracted, retrotranscribed, and the expressions of mouse *Il1b*, *Il6*, and *Inos* (5′-CAGCTGGGCTGTACAAACCTT-3′ and 5′-CATTGGAAGTGAAGCGTTTCG-3′) were quantified relative to *Gapdh* by quantitative PCR as described above.

Results

Antiangiogenic HGR-Containing Vasoinhibin Analogues Are Not Apoptotic, Inflammatory, or Fibrinolytic

The linear– (Vi45-51) and cyclic retro-inverse– (CRIVi45-51) HGR-containing vasoinhibin analogues, like vasoinhibin standards of 123 residues (Vi1-123) and 48-residues (Vi1-48) (Fig. 1A), inhibited the VEGF- and bFGF-induced proliferation of HUVEC (Fig. 1B) and the VEGF-induced invasion of HUVEC (Fig. 1C) without affecting the basal levels. These results confirm the antagonistic properties of HGR-containing vasoinhibin analogues (14) and serve to validate their use to explore other vasoinhibin actions. PRL is not antiangiogenic (10) and was used as a negative control.

Contrary to the 2 vasoinhibin isoforms (Vi1-123 and Vi1-48), the HGR-containing vasoinhibin analogues failed to induce the apoptosis and inflammatory phenotype of HUVEC as well as the lysis of a fibrin clot (Fig. 1D-1G). Vi1-123 and Vi1-48, but not Vi45-51, CRIVi45-51, or PRL, stimulated the apoptosis of HUVEC revealed by DNA fragmentation measured by ELISA (Fig. 1D), the adhesion of peripheral blood leukocytes to HUVEC monolayers (Fig. 1E), and the in vitro lysis of a plasma clot (Fig. 1F and 1G). Once the clot is formed (time 0), adding the thrombolytic agent tPA stimulates clot lysis, an action prevented by the co-addition of PAI-1. PAI-1 inhibition was reduced by Vi1-123 and Vi1-48 but not by Vi45-51, CRIVi45-51, or PRL (Fig. 1F and 1G). Because binding to PAI-1 mediates the fibrinolytic properties of vasoinhibin (23), the binding capacity to PAI-1 was evaluated by adding PAI-1 to ELISA plates coated with or without PRL, Vi1-123, Vi1-48, Vi45-51, or CRIVi45-51. The absorbance of the HRP-labeled antibody-PAI-1 complex increased only in the presence of Vi1-123 and Vi1-48 but not in uncoated wells and wells coated with the 2 HGR-containing vasoinhibin analogues or with PRL (Fig. 1H).

These findings show that the HGR-containing vasoinhibin analogues lack the apoptotic, inflammatory, and fibrinolytic properties of vasoinhibin. The fact that PRL is not inflammatory, apoptotic, or fibrinolytic indicates that, like the antiangiogenic effect (14), these vasoinhibin properties emerge upon PRL cleavage.

HGR-Containing Vasoinhibin Analogues Do Not Stimulate the Nuclear Translocation of NF-κB and the Expression of Inflammatory Molecules in HUVEC

Because vasoinhibin signals through NF-κB to induce the apoptosis and inflammation of endothelial cells (11, 12), we asked whether HGR-containing vasoinhibin analogues were able to promote the nuclear translocation of NF-κB and the expression of proinflammatory mediators in HUVEC (Fig. 2). The distribution of NF-κB in HUVEC was studied using fluorescence immunocytochemistry and monoclonal antibodies against the p65 subunit of NF-κB (Fig. 2A). Without treatment, p65 was homogeneously distributed throughout the cytoplasm of cells. Treatment with Vi1-123 or Vi1-48, but not with Vi45-51, CRIVi45-51, or PRL, resulted in the accumulation of p65 positive stain in the cell nucleus (Fig. 2A) indicative of the NF-κB nuclear translocation/activation needed for transcription. Consistently, only vasoinhibin isoforms (Vi1-123 or Vi1-48) and not the HGR-containing vasoinhibin analogues nor PRL induced the mRNA expression of genes encoding leukocyte adhesion molecules (intercellular adhesion molecule 1 [*ICAM1*] and vascular cell adhesion molecule 1 [*VCAM1*]) and proinflammatory cytokines (IL-1α (*IL1A*), IL-1β (*IL1B*), IL-6 (*IL6*), and tumor necrosis factor α [*TNF*]) in HUVEC (Fig. 2B). These findings show that HGR-containing vasoinhibin analogues are unable to activate NF-κB to promote gene transcription, resulting in the apoptosis and inflammation of HUVEC. Furthermore, these results suggest that a structural determinant—different from the HGR motif—is responsible for these properties.

Oligopeptides Containing the HNLSSEM Vasoinhibin Sequence Are Inflammatory, Apoptotic, and Fibrinolytic

Because the vasoinhibin of 48 residues (Vi1-48) conserves the apoptotic, inflammatory, and fibrinolytic properties of the larger vasoinhibin isoform (Vi1-123) (15), we scanned the sequence of the 48-residue isoform with synthetic oligopeptides (Fig. 3A) for their ability to stimulate the apoptosis and inflammation of HUVEC and the lysis of a fibrin clot. First, we confirmed that only the oligopeptide containing the HGR motif (35-48) inhibited the proliferation and invasion of HUVEC, whereas the oligopeptides lacking the HGR motif were not antiangiogenic (Fig. 3B and 3C).

Only the oligopeptides 20-35 and 30-45 promoted the apoptosis of HUVEC (Fig. 3D) and the leukocyte adhesion to HUVEC monolayers (Fig. 3E and 3F) like Vi1-123 and Vi1-48. The estimated potency (EC_{50}) of these oligopeptides was 800 pM, with a significantly higher effectiveness for the 30-45 oligopeptide (Fig. 3F). Likewise, the 20-35 and 30-45 oligopeptides, but not oligopeptides 1-15, 12-25, or 35-48, exhibited fibrinolytic properties (Fig. 3G and 3H) and bound PAI-1 like Vi1-123 and Vi1-48 (Fig. 3I). The shared sequence between the 20-35 and 30-45 oligopeptides corresponds to His30-Asn31-Leu32-Ser33-Ser34-Glu35 (HNLSSE) (Fig. 3A). However, the significantly higher effect of 30-45 over 20-35 in apoptosis, inflammation, fibrinolysis, and PAI-1 binding, suggests that the Met36 could be a part of the apoptotic, inflammatory, and fibrinolytic linear determinant of vasoinhibin (HNLSSEM).

Oligopeptides Containing the HNLSSEM Vasoinhibin Sequence Stimulate the Nuclear Translocation of NF-κB and the Expression of Inflammatory Factors in HUVEC

Consistent with their apoptotic and inflammatory effects, the 20-35 and the 30-45 oligopeptides, like vasoinhibin (Vi1-123 and Vi1-48), induced the nuclear translocation of NF-κB

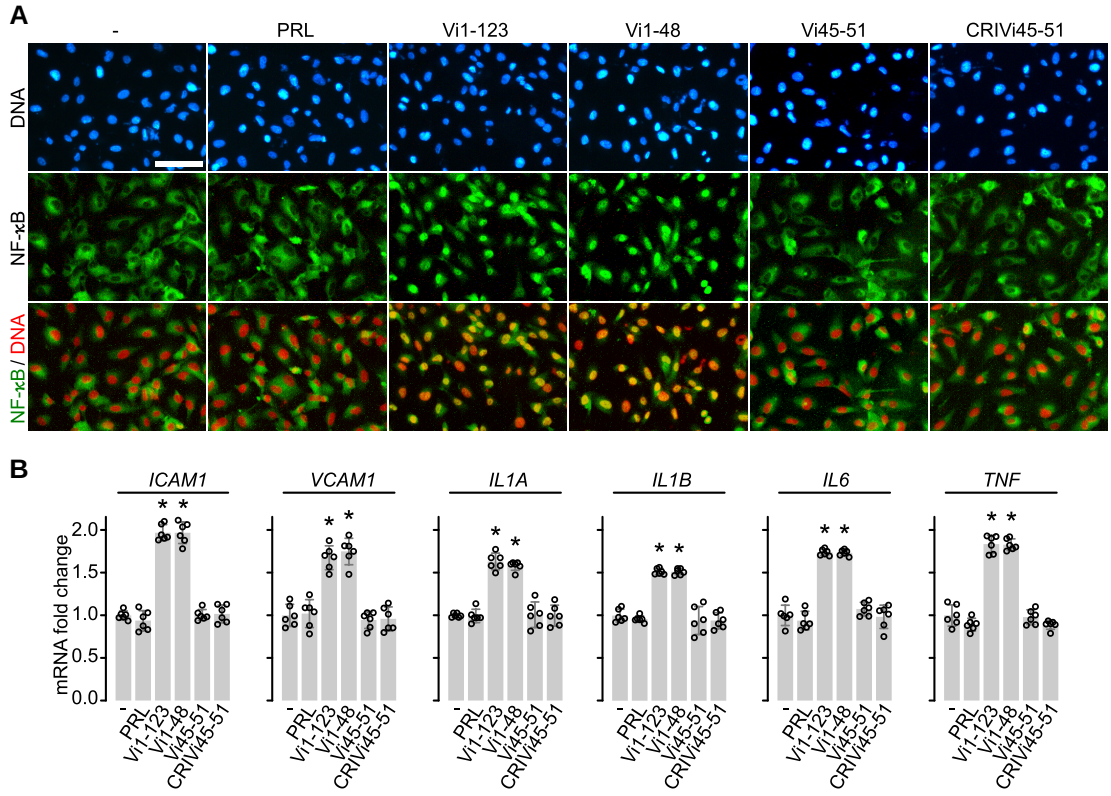

Figure 2. HGR-containing vasoinhibin analogues neither promote the nuclear translocation of NF-κB nor induce the expression of proinflammatory (A) immunofluorescence detection of NF-κB (p65) in HUVEC incubated in the absence (–) or presence of 100 nM of prolactin (PRL), the 123-residue (Vi1-123) and 48-residue (Vi1-48) vasoinhibin isoforms, and the linear (Vi45-51) and cyclic retro-inverse- (CRIVi45-51) HGR-containing vasoinhibin analogues. Scale bar = 100 µm. (B) HUVEC mRNA levels of cell adhesion molecules (*ICAM1* and *VCAM1*) and cytokines (*IL1A, IL1B, IL6,* and *TNF*) after incubation with or without (–) 100 nM of PRL, Vi1-123, Vi1-48, Vi45-51, or CRIVi45-51. Individual values are shown with open circles. Values are means ± SD of at least 3 independent experiments, $n = 6$, $^*P < .001$ vs control without treatment (–) (1-way ANOVA, Dunnett's).

(Fig. 4A) and upregulated the mRNA expression levels of the leukocyte adhesion molecules (*ICAM1* and *VCAM1*) and inflammatory cytokines (*IL1A*, *IL1B*, *IL6*, and *TNF*) genes in HUVEC (Fig. 4B).

In Vivo Inflammation Is Stimulated by the HNLSSEM Sequence and Not by the HGR Motif

To evaluate whether the HGR or the HNLSSEM motifs promotes the inflammatory phenotype of endothelial cells in vivo, the HGR-containing vasoinhibin analogue Vi45-51 or the HNLSSEM-containing 30-45 oligopeptide was injected intravenously to reach an estimated ≃10 µM concentration in serum, and after 2 hours, mice were perfused, and lung, liver, kidney, and eyes were collected to evaluate mRNA expression of leukocyte adhesion molecules (*Icam1* and *Vcam1*) and cytokines (*Il1b*, *Il6*, and *Tnf*), and the level of leukocyte marker (*Cd45*). The underlying rationale is that intravenous delivery and short-term (2-hour) analysis in thoroughly perfused animals would reflect a direct effect of the treatments on endothelial cell mRNA expression of inflammatory factors in the various tissues. The 30-45 peptide, but not the Vi45-51, increased the expression levels of these inflammatory markers in the evaluated tissues (Fig. 5A-5D). Furthermore, because vasoinhibin is inflammatory in joint tissues (24), we injected into the knee cavity of mice 87 pmol of the Vi45-51 or the 30-45 peptide, and after 24 hours, only the 30-45 oligopeptide induced the mRNA expression of *Il1b*, *Il6*, and inducible nitric oxide synthetase (*Inos*) (Fig. 5E). The finding in joints implied that, like vasoinhibin, the inflammatory effect of the 30-45 peptide extends to other vasoinhibin target cells, that is, synovial fibroblasts (24).

PAI-1, uPAR, and NF-κB Mediate the Apoptotic and Inflammatory Effects of the HNLSSEM Vasoinhibin Determinant

Vasoinhibin binds to a multimeric complex in endothelial cell membranes formed by PAI-1, uPA, and uPA receptor (uPAR) (PAI-1-uPA-uPAR) (23), but it is unclear whether such binding influences vasoinhibin-induced activation of NF-κB, the main signaling pathway mediating its apoptotic and inflammatory actions (11, 12, 25). Because the HNLSSEM determinant in vasoinhibin binds to PAI-1, activates NF-κB signaling, and stimulates the apoptosis and inflammation of HUVEC, we investigated their functional interconnection by testing whether inhibitors of PAI-1, uPAR, or NF-κB modified the apoptosis and leukocyte adhesion to HUVEC treated with Vi1-123 and the oligopeptides 20-35 and 30-45 (Fig. 6). Antibodies against uPAR and the inhibitor of NF-κB (BAY117085), but not the immunoneutralization of PAI-1, prevented the apoptotic effect of vasoinhibin and the HNLSSE-containing oligopeptides (Fig. 6A). In contrast, all 3 inhibitors prevented the adhesion of leukocytes to HUVEC in response to Vi1-123, 20-35, and 30-45 (Fig. 6B). These results indicate that vasoinhibin, through the HNLSSEM motif, uses PAI-1, uPAR, and/or NF-κB to mediate endothelial cell apoptosis and inflammation (Fig. 6C).

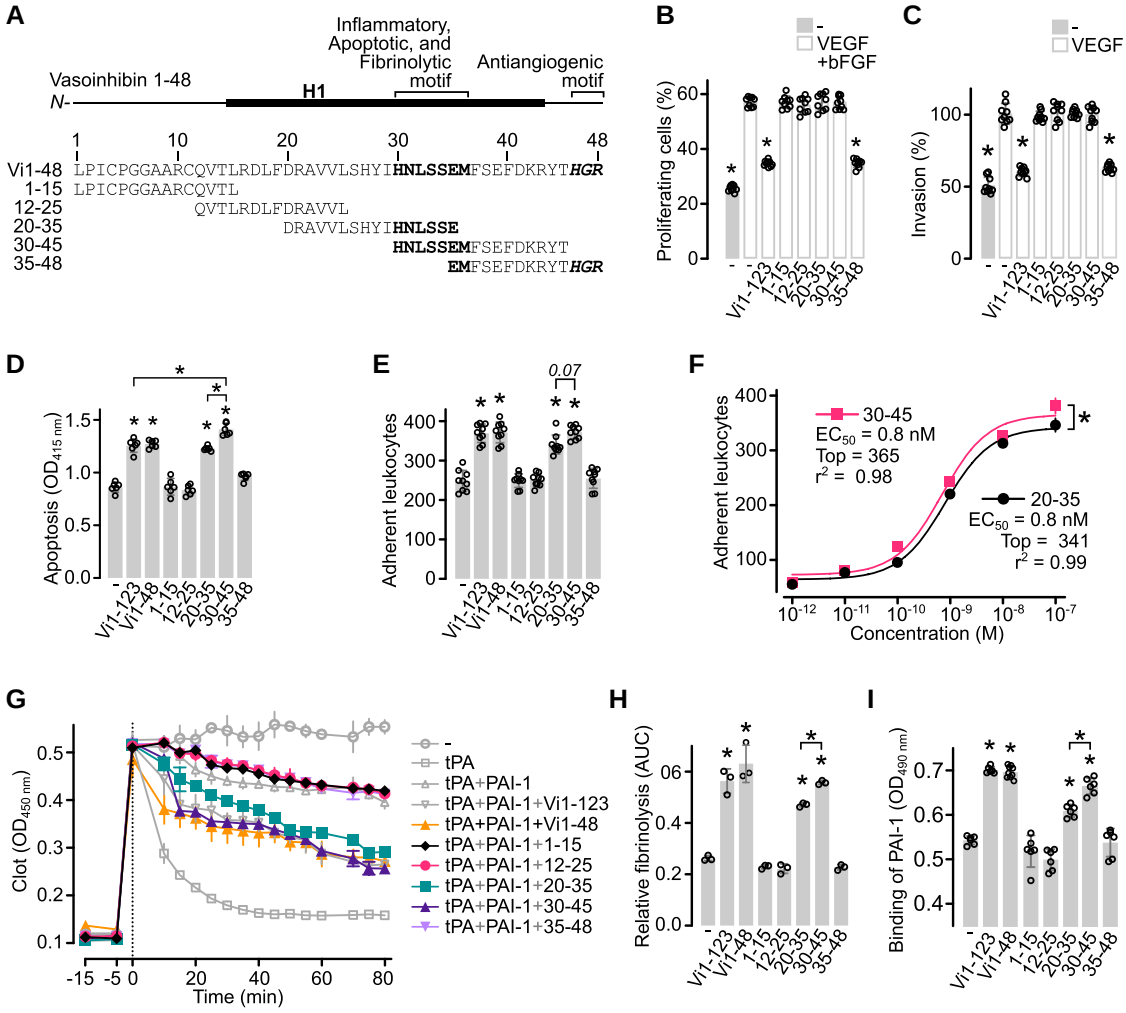

Figure 3. Oligopeptides containing the HNLSSEM sequence are inflammatory, apoptotic, and fibrinolytic. (A) Diagram of the sequence and localization of the oligopeptides scanning the 48-residue vasoinhibin isoform (Vi1-48). The α-helix 1 (H1), the inflammatory, apoptotic, and fibrinolytic sequence (HNLSSEM), and the antiangiogenic HGR motif are highlighted in bold. (B) Effect of 100 nM 123-residue vasoinhibin isoform (Vi1-123) or the scanning oligopeptides on the proliferation of HUVEC stimulated with 25 ng mL^{-1} of VEGF and 20 ng mL^{-1} of bFGF. Values are means ± SD relative to total cells (n = 9). (C) Effect of 100 nM Vi1-123 or the scanning oligopeptides on the invasion of HUVEC stimulated with 50 ng mL^{-1} of VEGF. Values are means ± SD relative to VEGF stimulated values (*n* = *9*). **P* < .0001 vs VEGF + bFGF (–) or VEGF (–) controls. (D) Effect of 100 nM of Vi1-123, Vi1-48, or the scanning oligopeptides on HUVEC apoptosis (*n* = *6*). (E) Effect of 100 nM of Vi1-123, Vi1-48, or the scanning oligopeptides on the leukocyte adhesion to a HUVEC monolayer (*n* = *9*). (F) Dose-response of the leukocyte adhesion to HUVEC after treatment with the 20-35 or the 30-45 oligopeptides. Curves were fitted by least square regression analysis (*n* = *6*, **P* = .02, paired *t* test). (G) Lysis of a plasma clot by tissue plasminogen activator (tPA) alone or together with plasminogen activator inhibitor-1 (PAI-1) in the presence or absence of Vi1-123, Vi1-48, or the scanning oligopeptides (*n* = *3*). (H) Fibrinolysis relative to tPA and tPA + PAI-1 calculated with the area under the curve (AUC) of (G). (I) Binding of PAI-1 to the immobilized Vi1-123, Vi1-48, or scanning oligopeptides in an ELISA-based assay (*n* = *6*). Individual values are shown with open circles. Values are means ± SD of at least 3 independent experiments, **P* < .001 vs without treatment (–) controls (1-way ANOVA, Dunnett's).

Discussion

Vasoinhibin represents a family of proteins comprising the first 48 to 159 amino acids of PRL, depending on the cleavage site of several proteases, including matrix metalloproteases (26), cathepsin D (27), bone morphogenetic protein 1 (28), thrombin (15), and plasmin (29). The cleavage of PRL occurs at the hypothalamus, the pituitary gland, and the target tissue levels, defining the PRL/vasoinhibin axis (30). This axis contributes to the physiological restriction of blood vessels in ocular (31, 32) and joint (26) tissues and is disrupted in angiogenesis-related diseases, including diabetic retinopathy (33), retinopathy of prematurity (34), peripartum cardiomyopathy (35), preeclampsia (36), and inflammatory arthritis (37). Furthermore, 2 clinical trials have addressed vasoinhibin levels as targets of therapeutic interventions (38). However, the clinical translation of vasoinhibin is limited by difficulties in its production (39). These difficulties were recently overcome by the development of HGR-containing vasoinhibin analogues that are easy to produce, as well as potent, stable, and even orally active to inhibit the growth and permeability of blood vessels in experimental vasoproliferative retinopathies and cancer (14). Nonetheless, the therapeutic value of HGR analogues is challenged by evidence showing that vasoinhibin is also apoptotic, inflammatory, and fibrinolytic, properties that may worsen microvascular diseases (40, 41). Here, we show that the various functions of vasoinhibin are segregated into 2 distinct, nonadjacent, and independent small linear motifs: the HGR motif responsible for the vasoinhibin inhibition of angiogenesis and vasopermeability (14) and the HNLSSEM motif responsible for the apoptotic, inflammatory, and fibrinolytic properties of vasoinhibin (Fig. 7A).

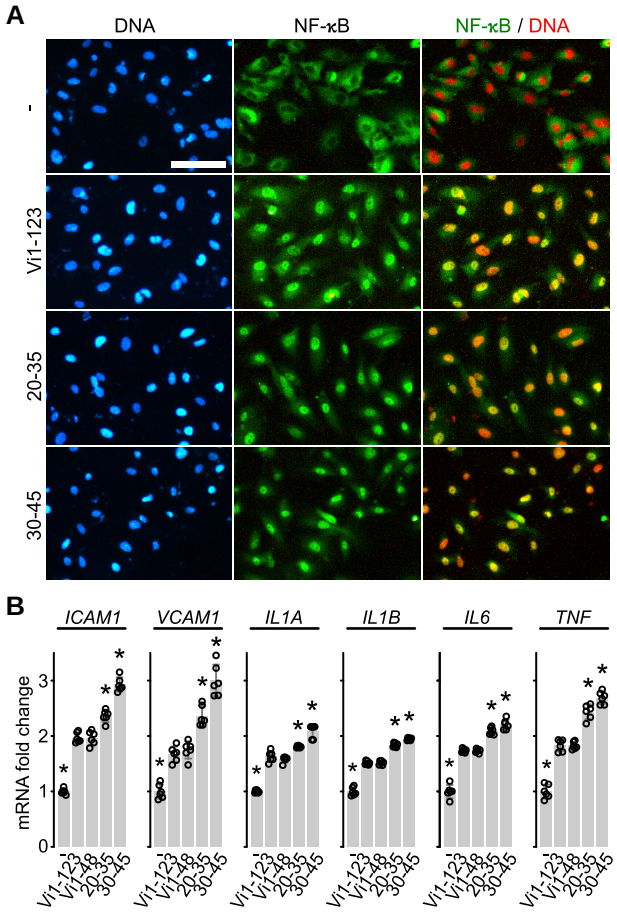

Figure 4. HNLSSEM-containing oligopeptides promote the nuclear translocation of NF-κB and induce the expression of proinflammatory genes (A) immunofluorescence detection of NF-κB (p65) in HUVEC incubated in the absence (–) or presence of 100 nM of the 123-residue vasoinhibin (vi1-123), the 20-35 or the 30-45 residue-oligopeptides. Scale bar = 100 µm. Micrographs are representative of 3 independent experiments. (B) HUVEC mRNA levels of cell adhesion molecules (*ICAM1* and *VCAM1*) and cytokines (*IL1A, IL1B, IL6,* and *TNF*) after incubation with or without (–) 100 nM of Vi1-123, Vi1-48, 20-35, or 30-45. Individual values are shown with open circles. Values are means ± SD, $n = 6$, $^*P < .001$ vs without treatment (–) controls (1-way ANOVA, Dunnett's).

The HGR and HNLSSEM motifs are inactive in PRL, the vasoinhibin precursor. We confirmed that PRL has no antiangiogenic properties (10) and showed that PRL lacks apoptotic and inflammatory actions on endothelial cells as well as no fibrinolytic activity. PRL has 199 amino acids structured into a 4-α-helix bundle topology connected by 3 loops (43). The HGR motif is in the first part of loop 1 (L1) connecting α-helixes 1 and 2, whereas the HNLSSEM motif is in α-helix 1 (H1) (Fig. 7A). Upon proteolytic cleavage, PRL loses its fourth α-helix (H4), which drives a conformational change and the exposure of the HGR motif, obscured by H4 (14, 42). Since H1 and H4 are in close contact in PRL (43), it is likely that some elements of H4 also mask the HNLSSEM motif. Alternatively, it is also possible that residues of the HNLSSEM motif buried in the hydrophobic core of PRL become solvent exposed by the conformational change into vasoinhibin. However, this is unlikely since the hydrophobic core appears conserved during vasoinhibin generation (42).

A previous report indicated that binding to PAI-1 mediates the antiangiogenic actions of vasoinhibin (23). Contrary to this claim, antiangiogenic HGR-containing vasoinhibin analogues did not bind PAI-1, whereas the HNLSSEM-oligopeptides bound PAI-1 but did not inhibit HUVEC proliferation and invasion. While these findings unveil the structural determinants in vasoinhibin responsible for PAI-1 binding, they question the role of PAI-1 as a necessary element for the antiangiogenic effects of vasoinhibin. Little is known of the molecular mechanism by which vasoinhibin binding to the PAI-1-uPA-uPAR complex inhibits endothelial cells (23). Although the binding could help localize vasoinhibin on the surface of endothelial cells, the contribution of other vasoinhibin-binding proteins and/or interacting molecules cannot be excluded. For example, integrin α5β1 interacts with the uPA-uPAR complex (44), and vasoinhibin binds to α5β1 to promote endothelial cell apoptosis (45). Nevertheless, none of the HGR-containing analogues induced apoptosis. Therefore, the binding molecule/receptor that transduces the antiangiogenic properties of vasoinhibin remains unclear.

Vasoinhibin is commonly described as antiangiogenic due to its ability to inhibit endothelial cell proliferation, migration, and survival. However, the proapoptotic effect of vasoinhibin can occur independent of its antiangiogenic action. For example, vasoinhibin contributes to the physiological regression by apoptosis of the stable hyaloid vasculature, a transient network of intraocular vessels that nourishes the immature lens, retina, and vitreous (46). Moreover, despite lacking proapoptotic properties, Vi45-51 inhibits the growth of melanoma tumors (14) like whole vasoinhibin (23, 47-49), to suggest that the apoptotic effect of vasoinhibin may be irrelevant to its overall antiangiogenic efficacy.

Consistent with previous reports (11, 12, 23), vasoinhibin binding to PAI-1 and activation of uPAR and NF-κB did associate with the apoptotic, inflammatory, and fibrinolytic properties of the HNLSSEM-containing oligopeptides. These oligopeptides, but not HGR-containing oligopeptides, induced endothelial cell apoptosis, nuclear translocation of NFκB, expression of leukocyte adhesion molecules and proinflammatory cytokines, and adhesion of leukocytes, as well as the lysis of plasma fibrin clot. The inflammatory action, but not the apoptotic effect, was prevented by PAI-1 immunoneutralization, whereas both inflammatory and apoptotic actions were blocked by anti-uPAR antibodies or by an inhibitor of NF-κB. Locating the apoptotic, inflammatory, and fibrinolytic activity in the same short linear motif of vasoinhibin is not unexpected since the 3 events can be functionally linked. The degradation of a blood clot is an important aspect of inflammatory responses, and major components of the fibrinolytic system are regulated by inflammatory mediators (50). Examples of such interactions are the thrombin-induced generation of vasoinhibin during plasma coagulation to promote fibrinolysis (15), the endotoxin-induced IL-1 production inhibited by PAI-1 (51), and the TNFα-induced suppression of fibrinolytic activity due to the activation of NFκB-mediated PAI-1 expression (52). Furthermore, uPA is upregulated by thrombin and inflammatory mediators in endothelial cells (53), and uPAR is elevated under inflammatory conditions (54). On the other hand, the identification of HNLSSEM as the motif responsible for the binding of vasoinhibin to PAI-1 raises the possibility that such motif contributes to the interaction of other proteins with PAI-1, like vitronectin, uPA, and tPA (55). Our preliminary analyses found no identical HNLSSEM sequences in these proteins but detected similar motifs in regions shown to be irrelevant for binding to PAI-1 that merit further research.

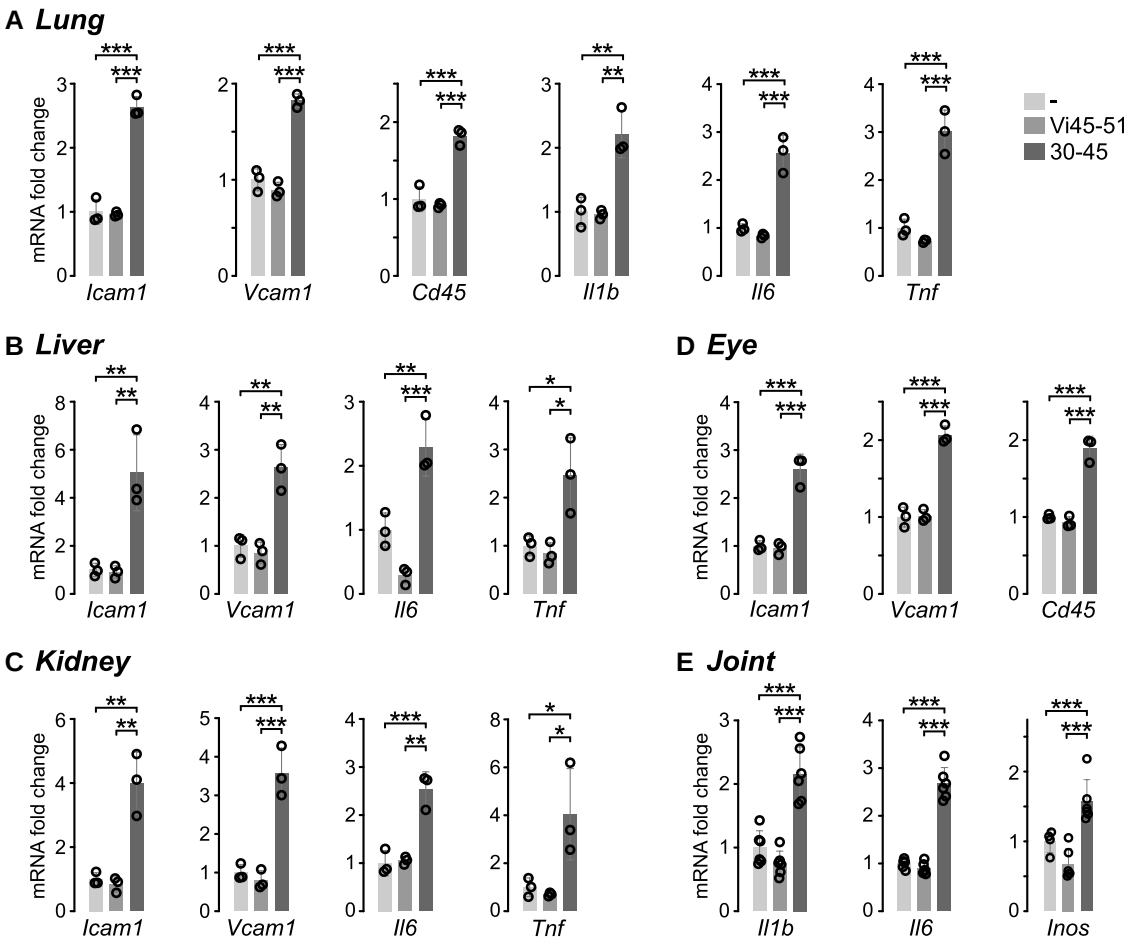

Figure 5. The HNLSSEM motif, but not the HGR motif, stimulates inflammation in vivo. Expression mRNA levels of adhesion molecules (*Icam1* and *Vcam1*), a leukocyte marker (*Cd45*), and cytokines (*Il1b*, *Il6*, and *Tnf*) in lung (A), liver (B), kidney (C), and eye (D) from mice after 2 hours of intravenous injection of 16.6 μg of the HGR-containing vasoinhibin analogue Vi45-51 or 40.7 μg of the HNLSSEM-containing 30-45 oligopeptide. (E) Expression mRNA levels of IL-1β, IL-6, and iNOS in knee joints of mice 24 hours after the intra-articular injection of 72 ng of Vi45-51 or 176.8 ng of the 30-45 oligopeptide. Values are means ± SD, $n = 3$, *$P < .033$, **$P < .002$, ***$P < .001$ (1-way ANOVA, Tukey's).

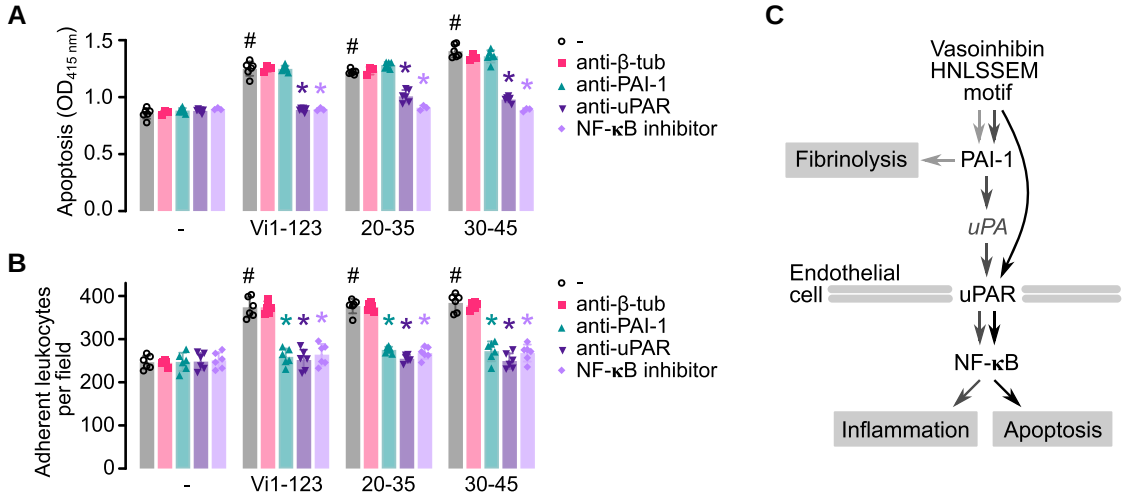

Figure 6. Inhibition of PAI-1, uPAR, and NF-κB signaling prevents the apoptotic and inflammatory effects of the HNLSSEM motif. Apoptosis of HUVEC (A) and leukocyte adhesion to a HUVEC monolayer (B) in response to the 123-residue vasoinhibin isoform (Vi1-123), the HNLSSEM-containing 20-35 or 30-45 oligopeptides in the absence (–) or presence of antibodies against β-tubulin (anti-β-tub), PAI-1 (anti-PAI-1), or uPAR (anti-uPAR), or the NF-κB inhibitor BAY117085. Values are means ± SD, $n \geq 3$, #$P < .001$ vs respective untreated (–) group, *$P < .0001$ vs absence of antibodies (–) (2-way ANOVA, Dunnett's). (C) Schematic representation to illustrate that the HNLSSEM motif promotes fibrinolysis by binding to PAI-1 and endothelial cell apoptosis and inflammation via the activation of uPAR and NF-κB.

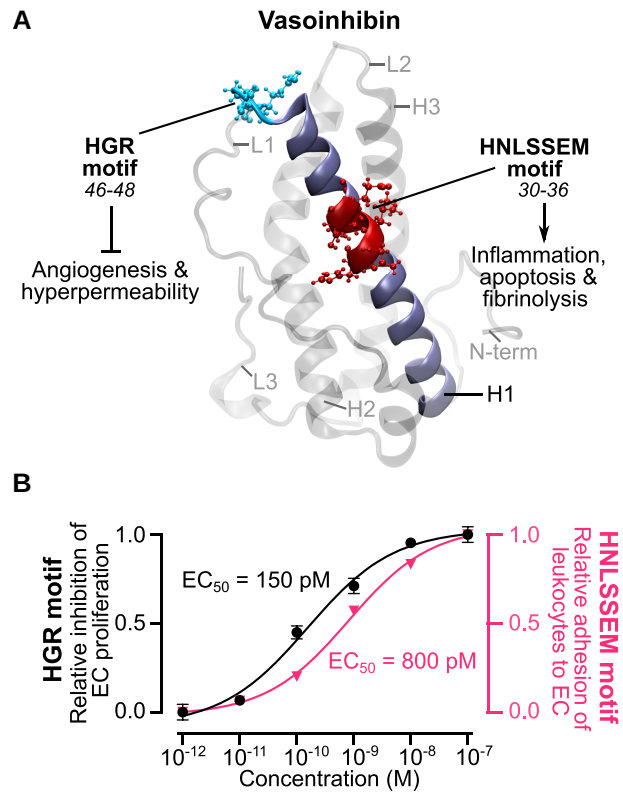

Figure 7. Vasoinhibin properties are segregated into 2 independent motifs. (A) The vasoinhibin inhibitory properties on angiogenesis and vasopermeability are in the HGR motif (cyan), comprising residues 46 to 48, located in the early part of loop 1 (L1), whereas the inflammatory, apoptotic, and fibrinolytic properties of vasoinhibin reside in the HNLSSEM motif (red), comprising residues 30 to 36, located at the middle of α-helix 1 (H1) (navy blue). The vasoinhibin model was previously reported (42), and the figure was generated with Visual Molecular Dynamics software. (B) Comparison of the dose-response curves showing the relative inhibition of endothelial cell proliferation by the HGR-containing analogue Vi45-51 (14) and the relative stimulation of leukocyte adhesion to endothelial cells by the HNLSSEM-containing peptide 30-45 (Fig. 3F). Curves were fitted by least square regression analysis ($n \geq 6$).

The HNLSSEM-oligopeptides' inflammatory action is further supported by their in vivo administration. The intravenous injection of HNLSSEM-oligopeptides upregulated the short-term (2 hours postinjection) expression of *Icam1* and *Vcam1*, *Il1b*, *Il6*, and *Tnf*, and the infiltration of leukocytes (evaluated by the expression levels of the leukocyte marker *Cd45*) in different tissues indicative of an inflammatory action on different vascular beds. Also, the HNLSSEM-oligopeptides injected into the intra-articular space of joints launched a longer-term inflammation (24 hours postinjection) indicative of an inflammatory response in joint tissues. This action is consistent with the vasoinhibin-induced stimulation of the inflammatory response of synovial fibroblasts, primary effectors of inflammation in arthritis (37).

The challenge is to understand when and how vasoinhibin impacts angiogenesis, apoptosis, inflammation, and fibrinolysis pathways under health and disease. One likely example is during the physiological repair of tissues after wounding and inflammation. By inhibiting angiogenesis, vasoinhibin could help counteract the proangiogenic action of growth factors and cytokines, whereas by stimulating apoptosis, inflammation, and fibrinolysis, vasoinhibin could promote the pruning of blood vessels, protective inflammatory reactions, and clot dissolution needed for tissue remodeling. Indeed, the antiangiogenic effect of vasoinhibin can be accompanied by its inflammatory actions. Although, the HNLSSEM motif has 5.3 times less potency than the HGR motif (Fig. 7B). However, in the absence of successful containment, overproduction of blood vessels, persistent inflammation, and dysfunctional coagulation determines the progression and therapeutic outcomes in cancer (41, 56), diabetic retinopathy (57), and rheumatoid arthritis (58). The complexity of vasoinhibin actions under disease is exemplified in murine antigen-induced arthritis, where vasoinhibin ameliorates pannus formation and growth via an antiangiogenic mechanism but promotes joint inflammation by stimulating the inflammatory response of synovial fibroblasts (37, 59).

Antiangiogenic drugs, in particular VEGF inhibitors, have reached broad usage in the field of cancer and retinopathy, albeit with partial success and safety concerns (6, 60, 61). They display modest efficacy and survival times, resistance, and mild to severe side effects that include infections, bleeding, wound healing complications, and thrombotic events. Toxicities illustrate the association between the inhibition of blood vessel growth and multifactorial pathways influencing endothelial cell apoptosis, inflammation, and coagulation (6). The fact that the HGR analogues lack the apoptotic, inflammatory, and fibrinolytic properties of vasoinhibin highlights their future as potent and safe inhibitors of blood vessel growth, avoiding drug resistance through their broad action against different proangiogenic substances.

In summary, this work segregates the activities of vasoinhibin into 2 linear determinants and provides clear evidence that the HNLSSEM motif is responsible for binding to PAI-1 and exerting apoptotic, inflammatory, and fibrinolytic actions via PAI-1, uPAR, and NF-κB pathways, while the HGR motif is responsible for the antiangiogenic effects of vasoinhibin. This knowledge provides tools for dissecting the differential effects and signaling mechanisms of vasoinhibin under health and disease and for improving its development into more specific, potent, and less toxic antiangiogenic, proinflammatory, and fibrinolytic drugs.

Acknowledgments

We thank Xarubet Ruíz Herrera, Fernando López Barrera, Adriana González Gallardo, Alejandra Castilla León, José Martín García Servín, and María A. Carbajo Mata for their excellent technical assistance.

Funding

The work was supported by grant A1-S-9620B from Consejo Nacional de Humanidades, Ciencias y Tecnologias (CONAHCYT) and grant SECTEI/061/2023 from Secretaría de Educación, Ciencia, Tecnología e Innovación de la Ciudad de México (SECTEI) to C.C. and CF-2023-I-113 grant from CONAHCYT to G.M.E.

Disclosures

The authors declare the following broadly competing interests: J.P.R., M.Z., T.B., G.M.E., J.T., and C.C. are inventors of a submitted patent application (WO/2021/098996). The

Universidad Nacional Autónoma de México (UNAM) and the authors J.T. and T.B. are owners of the pending patent. J.P.R. is the CEO and Founder of VIAN Therapeutics, Inc.

Data Availability

Original data generated and analyzed during this study are included in this published article or in the data repositories listed in References.

References

1. Carmeliet P. Angiogenesis in health and disease. *Nat Med*. 2003;9(6):653-660.
2. Qin S, Li A, Yi M, Yu S, Zhang M, Wu K. Recent advances on anti-angiogenesis receptor tyrosine kinase inhibitors in cancer therapy. *J Hematol Oncol*. 2019;12(1):27.
3. Gotink KJ, Verheul HMW. Anti-angiogenic tyrosine kinase inhibitors: what is their mechanism of action? *Angiogenesis*. 2010;13(1):1-14.
4. Apte RS, Chen DS, Ferrara N. VEGF in signaling and disease: beyond discovery and development. *Cell*. 2019;176(6):1248-1264.
5. Fallah A, Sadeghinia A, Kahroba H, *et al*. Therapeutic targeting of angiogenesis molecular pathways in angiogenesis-dependent diseases. *Biomed Pharmacother*. 2019;110:775-785.
6. Verheul HMW, Pinedo HM. Possible molecular mechanisms involved in the toxicity of angiogenesis inhibition. *Nat Rev Cancer*. 2007;7(6):475-485.
7. Widakowich C, de Castro G Jr, de Azambuja E, Dinh P, Awada A. Review: side effects of approved molecular targeted therapies in solid cancers. *Oncologist* 2007;12(12):1443-1455.
8. Xu H, Zhao G, Yang J, Wen X. Advances in toxicity risk analysis and effective treatments for targeted antiangiogenic drugs. *Int J Clin Exp Med*. 2019;12(10):12020-12027.
9. Bergers G, Hanahan D. Modes of resistance to anti-angiogenic therapy. *Nat Rev Cancer*. 2008;8(8):592-603.
10. Clapp C, Thebault S, Macotela Y, Moreno-Carranza B, Triebel J, Martinez de la Escalera G. Regulation of blood vessels by prolactin and vasoinhibins. *Adv Exp Med Biol*. 2015;846:83-95.
11. Tabruyn SP, Sorlet CM, Rentier-Delrue F, *et al*. The antiangiogenic factor 16 K human prolactin induces caspase-dependent apoptosis by a mechanism that requires activation of nuclear factor-kappaB. *Mol Endocrinol*. 2003;17(9):1815-1823.
12. Tabruyn SP, Sabatel C, Nguyen N-Q-N, *et al*. The angiostatic 16 K human prolactin overcomes endothelial cell anergy and promotes leukocyte infiltration via nuclear factor-kappaB activation. *Mol Endocrinol*. 2007;21(6):1422-1429.
13. Martini JF, Piot C, Humeau LM, Struman I, Martial JA, Weiner RI. The antiangiogenic factor 16 K PRL induces programmed cell death in endothelial cells by caspase activation. *Mol Endocrinol*. 2000;14(10):1536-1549.
14. Robles JP, Zamora M, Siqueiros-Marquez L, *et al*. The HGR motif is the antiangiogenic determinant of vasoinhibin: implications for a therapeutic orally active oligopeptide. *Angiogenesis*. 2022;25(1):57-70.
15. Zamora M, Robles JP, Aguilar MB, *et al*. Thrombin cleaves prolactin into a potent 5.6-kDa vasoinhibin: implication for tissue repair. *Endocrinology*. 2021;162(12):bqab177.
16. Galfione M, Luo W, Kim J, *et al*. Expression and purification of the angiogenesis inhibitor 16-kDa prolactin fragment from insect cells. *Protein Expr Purif*. 2003;28(2):252-258.
17. Keeler C, Dannies PS, Hodsdon ME. The tertiary structure and backbone dynamics of human prolactin. *J Mol Biol*. 2003;328(5):1105-1121.
18. Baudin B, Bruneel A, Bosselut N, Vaubourdolle M. A protocol for isolation and culture of human umbilical vein endothelial cells. *Nat Protoc*. 2007; 2(3):481-485.
19. Salic A, Mitchison TJ. A chemical method for fast and sensitive detection of DNA synthesis in vivo. *Proc Natl Acad Sci U S A*. 2008;105(7):2415-2420.
20. Carpenter AE, Jones TR, Lamprecht MR, *et al*. CellProfiler: image analysis software for identifying and quantifying cell phenotypes. *Genome Biol*. 2006;7(10):R100.
21. Justus CR, Leffler N, Ruiz-Echevarria M, Yang LV. In vitro cell migration and invasion assays. *J Vis Exp*. 2014;88(88):51046.
22. Robles JP, Zamora M, Adan-Castro E, Siqueiros-Marquez L, de la Escalera GM, Clapp C. The spike protein of SARS-CoV-2 induces endothelial inflammation through integrin α5β1 and NF-κB signaling. *J Biol Chem*. 2022;298(3):101695.
23. Bajou K, Herkenne S, Thijssen VL, *et al*. PAI-1 mediates the antiangiogenic and profibrinolytic effects of 16 K prolactin. *Nat Med*. 2014;20(7):741-747.
24. Ortiz G, Ledesma-Colunga MG, Wu Z, *et al*. Vasoinhibin is generated and promotes inflammation in mild antigen-induced arthritis. *Endocrinology*. 2022;163(5):bqac036.
25. Macotela Y, Mendoza C, Corbacho AM, *et al*. 16 K prolactin induces NF-kappaB activation in pulmonary fibroblasts. *J Endocrinol*. 2002;175(3):R13-R18.
26. Macotela Y, Aguilar MB, Guzman-Morales J, *et al*. Matrix metalloproteases from chondrocytes generate an antiangiogenic 16 kDa prolactin. *J Cell Sci*. 2006;119(9):1790-1800.
27. Piwnica D, Touraine P, Struman I, *et al*. Cathepsin D processes human prolactin into multiple 16K-like N-terminal fragments: study of their antiangiogenic properties and physiological relevance. *Mol Endocrinol*. 2004;18(10):2522-2542.
28. Ge G, Fernandez CA, Moses MA, Greenspan DS. Bone morphogenetic protein 1 processes prolactin to a 17-kDa antiangiogenic factor. *Proc Natl Acad Sci U S A*. 2007;104(24):10010-10015.
29. Friedrich C, Neugebauer L, Zamora M, *et al*. Plasmin generates vasoinhibin-like peptides by cleaving prolactin and placental lactogen. *Mol Cell Endocrinol*. 2021;538:111471.
30. Triebel J, Bertsch T, Bollheimer C, *et al*. Principles of the prolactin/vasoinhibin axis. *Am J Physiol Regul Integr Comp Physiol*. 2015;309(10):R1193-R1203.
31. Aranda J, Rivera JC, Jeziorski MC, *et al*. Prolactins are natural inhibitors of angiogenesis in the retina. *Invest Ophthalmol Vis Sci*. 2005;46(8):2947-2953.
32. Dueñas Z, Torner L, Corbacho AM, *et al*. Inhibition of rat corneal angiogenesis by 16-kDa prolactin and by endogenous prolactin-like molecules. *Invest Ophthalmol Vis Sci*. 1999;40(11):2498-2505.
33. Triebel J, Bertsch T, Clapp C. Prolactin and vasoinhibin are endogenous players in diabetic retinopathy revisited. *Front Endocrinol (Lausanne)*. 2022;13:994898.
34. Zepeda-Romero LC, Vazquez-Membrillo M, Adan-Castro E, *et al*. Higher prolactin and vasoinhibin serum levels associated with incidence and progression of retinopathy of prematurity. *Pediatr Res*. 2017; 81(3):473-479.
35. Hilfiker-Kleiner D, Kaminski K, Podewski E, *et al*. A cathepsin D-cleaved 16 kDa form of prolactin mediates postpartum cardiomyopathy. *Cell*. 2007;128(3):589-600.
36. Gonzalez C, Parra A, Ramirez-Peredo J, *et al*. Elevated vasoinhibins may contribute to endothelial cell dysfunction and low birth weight in preeclampsia. *Lab Invest*. 2007;87(10):1009-1017.
37. Clapp C, Ortiz G, García-Rodrigo JF, *et al*. Dual roles of prolactin and vasoinhibin in inflammatory arthritis. *Front Endocrinol (Lausanne)*. 2022;13:905756.
38. Triebel J, Robles-Osorio ML, Garcia-Franco R, Martinez de la Escalera G, Clapp C, Bertsch T. From bench to bedside: translating the prolactin/vasoinhibin axis. *Front Endocrinol (Lausanne)*. 2017;8:342.
39. Moreno-Carranza B, Robles JP, Cruces-Solís H, *et al*. Sequence optimization and glycosylation of vasoinhibin: pitfalls of recombinant production. *Protein Expr Purif*. 2019;161:49-56.
40. Forrester JV, Kuffova L, Delibegovic M. The role of inflammation in diabetic retinopathy. *Front Immunol*. 2020;11:583687.
41. Zhao H, Wu L, Yan G, *et al*. Inflammation and tumor progression: signaling pathways and targeted intervention. *Signal Transduct Target Ther*. 2021;6(1):263.

42. Robles JP, Zamora M, Velasco-Bolom JL, *et al.* Vasoinhibin comprises a three-helix bundle and its antiangiogenic domain is located within the first 79 residues. *Sci Rep*. 2018;8(1):17111.
43. Teilum K, Hoch JC, Goffin V, Kinet S, Martial JA, Kragelund BB. Solution structure of human prolactin. *J Mol Biol*. 2005;351(4):810-823.
44. Wei Y, Czekay R-P, Robillard L, *et al.* Regulation of α5β1 integrin conformation and function by urokinase receptor binding. *J Cell Biol*. 2005;168(3):501-511.
45. Morohoshi K, Mochinaga R, Watanabe T, Nakajima R, Harigaya T. 16 kDa vasoinhibin binds to integrin alpha5 beta1 on endothelial cells to induce apoptosis. *Endocr Connect*. 2018;7(5):630-636.
46. Duenas Z, Rivera JC, Quiroz-Mercado H, *et al.* Prolactin in eyes of patients with retinopathy of prematurity: implications for vascular regression. *Invest Ophthalmol Vis Sci*. 2004;45(7):2049-2055.
47. Nguyen NQ, Castermans K, Berndt S, *et al.* The antiangiogenic 16 K prolactin impairs functional tumor neovascularization by inhibiting vessel maturation. *PLoS One*. 2011;6(11):e27318.
48. Nguyen NQ, Cornet A, Blacher S, *et al.* Inhibition of tumor growth and metastasis establishment by adenovirus-mediated gene transfer delivery of the antiangiogenic factor 16 K hPRL. *Mol Ther*. 2007;15(12):2094-2100.
49. Kinet V, Nguyen NQ, Sabatel C, *et al.* Antiangiogenic liposomal gene therapy with 16 K human prolactin efficiently reduces tumor growth. *Cancer Lett*. 2009;284(2):222-228.
50. Medcalf RL. Fibrinolysis, inflammation, and regulation of the plasminogen activating system. *J Thromb Haemost*. 2007;5(s1):132-142.
51. Robson S, Saunders R, Kirsch R. Monocyte-macrophage release of IL-1 is inhibited by type-1 plasminogen activator inhibitors. *J Clin Lab Immunol*. 1990;33(2):83-90.
52. Hou B, Eren M, Painter CA, *et al.* Tumor necrosis factor α activates the human plasminogen activator inhibitor-1 gene through a distal nuclear factor κB site. *J Biol Chem*. 2004;279(18):18127-18136.
53. Wu S-Q, Aird WC. Thrombin, TNF-α, and LPS exert overlapping but nonidentical effects on gene expression in endothelial cells and vascular smooth muscle cells. *Am J Physiol Heart Circ Physiol*. 2005;289(2):H873-H885.
54. Slot O, Brünner N, Locht H, Oxholm P, Stephens RW. Soluble urokinase plasminogen activator receptor in plasma of patients with inflammatory rheumatic disorders: increased concentrations in rheumatoid arthritis. *Ann Rheum Dis*. 1999;58(8):488-492.
55. Arroyo De Prada N, Schroeck F, Sinner E-K, *et al.* Interaction of plasminogen activator inhibitor type-1 (PAI-1) with vitronectin. *Eur J Biochem*. 2002;269(1):184-192.
56. Elice F, Jacoub J, Rickles FR, Falanga A, Rodeghiero F. Hemostatic complications of angiogenesis inhibitors in cancer patients. *Am J Hematol*. 2008;83(11):862-870.
57. Murugesan N, Üstunkaya T, Feener EP. Thrombosis and hemorrhage in diabetic retinopathy: a perspective from an inflammatory standpoint. *Semin Thromb Hemost*. 2015;41(06):659-664.
58. Omair MA, Alkhelb SA, Ezzat SE, Boudal AM, Bedaiwi MK, Almaghlouth I. Venous thromboembolism in rheumatoid arthritis: the added effect of disease activity to traditional risk factors. *Open Access Rheumatol*. 2022;14:231-242.
59. Ortiz G, Ledesma-Colunga MG, Wu Z, *et al.* Vasoinhibin reduces joint inflammation, bone loss, and the angiogenesis and vasopermeability of the pannus in murine antigen-induced arthritis. *Lab Invest*. 2020;100(8):1068-1079.
60. Rust R, Gantner C, Schwab ME. Pro- and antiangiogenic therapies: current status and clinical implications. *FASEB J*. 2019;33(1):34-48.
61. Ghasemi Falavarjani K, Nguyen QD. Adverse events and complications associated with intravitreal injection of anti-VEGF agents: a review of literature. *Eye*. 2013;27(7):787-794. doi:10.1038/eye.2013.107